PHOTOPYROELECTRIC SPECTROSCOPY (P^2ES) OF

a-Si:H THIN SEMICONDUCTING FILMS ON QUARTZ

A. Mandelis, R.E. Wagner, K. Ghandi, and R. Baltman

Photoacoustic and Photothermal Sciences Laboratory
Department of Mechanical Engineering, and
Ontario Laser and Lightwave Research Center
University of Toronto, Toronto M5S 1A4, Canada

Phat Dao

Corporate Analytical Laboratory
Eastman Kodak Research Laboratories
Rochester, New York 14650

INTRODUCTION

Photopyroelectric Spectroscopy has proven to be a sensitive qualitative [1] and quantitative [2] technique for thin film spectroscopic applications. An important feature of this back-surface detection technique, not shared with the more conventional front-surface photothermal detection methods (Photothermal Deflection Spectroscopy, PDS; and Photoacoustic Spectroscopy, PAS) is its ability to measure *directly* and *separately* two independent spectrally-varying parameters: the optical absorption coefficient [3] and the nonradiative quantum efficiency. PDS of thin semiconducting films of amorphous hydrogenated *Si* [4] readily yields information about the *product* of the optical absorption coefficient, $\alpha(\lambda)$, and the nonradiative quantum efficiency, $\eta(\lambda)$. The standard assumption is, however, that $\eta(\lambda)$ is not a sensitive function of the exciting photon energy. This assumption is generally wrong, and nonradiative quantum efficiencies have been found photoacoustically to vary by one order of magnitude [5] across the optical gap in *Ge* doped $As_2\ Se_3$ chalcogenide glasses. PAS yields amorphous thin film spectra similar to PDS [6]. The working assumption has been that PA spectra are essentially accurate above the optical gap, as $\eta(\lambda)$ is expected to be independent of photon energy. Kitamura et al. [5] were able to derive extended $\eta(\lambda)$ spectra of $(As_2Se_3)_{100-x}\ Ge_x$ glasses upon combining PA spectra with optical absorption coefficient information obtained in an independent spectrophotometric experiment using ordinary polished bulk samples. These authors, however, were not able to guarantee that the glasses and the bulk samples had the same (or even nearly similar) $\alpha(\lambda)$ spectra.

From an experimental point of view, it is highly desirable to develop a thin film photothermal spectroscopic technique which can exhibit the convenience and high sensitivity of PDS without the requirement for a fluid intermediate with a large refractive index gradient $\partial n/\partial T$ (e.g. CCl_4 or water) where the probe beam may propagate and get deflected. The presence of the liquid interface in PDS precludes experimentation at low temperatures and may have electrochemical consequences in the case of ultrathin quantum well structures. In that case alternative interface waveguiding structures involving the contact of the epitaxial

side with a glass slide, have been employed [7]. Furthermore, in terms of detector noise limitations, PAS suffers from microphonic acoustic noise [8], and PDS is probe beam poynting noise limited [8,9]. P^2ES, on the other hand, operates on the pyroelectric principle and is not limited by the abovementioned noise sources. Finally, in our own experience, and that of others [10], three-dimensional effects associated with the location of the laser probe beam with respect to the dark edge of the illuminated sample surface region in a PDS experiment, have substantial influence on the PDS measurements. An alternative method insensitive, or less sensitive than PDS, to such geometrical constraints would appear desirable at this point in the evolution of thin-film photothermal spectroscopies. In this work we present our preliminary findings in the first application of P^2ES to a-*Si:H* thin film investigations and compare features of the obtained spectra to conventional PDS data.

THEORETICAL

The idealized geometry for P^2ES detection has been detailed elsewhere [1,3]. The detector element is assumed to be a PVDF thin pyroelectric film with opaque metal electrodes on both sides. The irradiating light is assumed to be modulated sinusoidally. Our specific geometry has been considered previously [1] and the complex P^2E signal response can be expressed as

$$\Delta V \equiv S(\lambda,\omega) = C(\omega) I_o(\lambda)\,[\eta_{Si}(\lambda) A_{Si}(\lambda) \exp[-(1+i) a_Q(\omega) d_Q] + A_F(\lambda)\eta_F(\lambda) T_{Si}(\lambda)] \quad (1)$$

In Eq. (1), $C(\omega)$ is an assortment of instrumental and geometric parameters of the sample-PVDF detector system; $\eta_{Si}(\lambda)$ and $\eta_F(\lambda)$ are the nonradiative quantum efficiencies of the a-*Si:H* thin film and the PVDF film detector, respectively; $A_{Si}(\lambda)$ and $T_{Si}(\lambda)$ are the *Si* absorptance and transmittance, respectively; and $a_Q(\omega)$, d_Q are the thermal diffusion coefficient and thickness of the quartz substrate. The former quantity is defined by $a_Q(\omega) = (\omega/2\beta_Q)^{1/2}$, where β_Q is the quartz thermal diffusivity. In the absence of the a-*Si:H* sample, the P^2E reference signal $S_R(\lambda,\omega)$ can be written as

$$\Delta V_{Ref} \equiv S_R(\lambda,\omega) = C(\omega) I_o(\lambda)\eta_F(\lambda) A_F(\lambda) \quad (2)$$

For the present purposes, the PVDF film absorptance, $A_F(\lambda)$, can be assumed to equal $1 - R_F(\lambda)$, where $R(\lambda)$ stands for the reflectance. i.e. the transmittance of the detector will be assumed to be zero, a very good approximation for electroded and coated thin film pyroelectric PVDF. Two special cases of the simple theory presented above are of experimental interest in the context of this work.

A. High Frequency Limit

This limit is defined by the thermally thick condition $a_Q(\omega) d_Q \gg 1$ or $f \gg \beta_Q/\pi d_Q^2$. Eqs. (1) and (2) then yield the normalized signal expression

$$S(\lambda,\omega) / S_R(\lambda,\omega) \approx T_{Si}(\lambda) \quad (3)$$

In this case, a wavelength scan will produce an optical transmission spectrum of the thin-film sample. For a thin absorbing a-*Si:H* film deposited on a non-absorbing substrate, at normal incidence, it is known that [11]

$$T_{Si}(\lambda) = 16 n_o n_Q (n^2 + k^2)/[BD\exp(\alpha d_{Si}) + EC\exp(-\alpha d_{Si}) + 2V\cos(4n\pi d_{Si}/\lambda) + 2U\sin(4n\pi d_{Si}/\lambda)] \quad (4)$$

where n_o is the index of refraction for air ($n_o = 1$), n_Q is the quartz index of refraction ($\approx n_{Glass} = 1.516$), and the a-*Si:H* thin film complex refractive index is given by $N(\lambda) = n(\lambda) - ik(\lambda)$, with the extinction

coefficient associated with the optical absorption coefficient through the relation $\alpha(\lambda) = 4\pi k(\lambda)/\lambda$. The remaining constants in Eq. (4) (i.e. B, C, D, E, U, and V) are functions of n, k, n_o, and n_Q. Furthermore, $n(\lambda)$ and $k(\lambda)$ are linked together through Eq. (4) and a similar non-linear expression [11] for the reflectance, $R(\lambda)$. No simple mathematical method exists for solving for $n(\lambda)$ and $k(\lambda)$ from the expressions for $T(\lambda)$ and $R(\lambda)$, however, several schemes have appeared in the literature with various degrees of success [12-15]. For the purpose of obtaining approximate P^2E spectra from experimental data through the optical gap region, the mathematically convenient Incoherent Approximation [16] may be used:

$$T(\lambda) = 16n^2 n_o n_Q/[BD\exp(\alpha d_{Si}) - CE\exp(-\alpha d_{Si})] \tag{5}$$

B. Low Frequency Limit

In this case the thermally thin condition $f \leq \beta_Q/\pi d_Q^2$ gives the following expression for the normalized signal:

$$\frac{S(\lambda,\omega)}{S_R(\lambda,\omega)} = \frac{\eta_{Si}(\lambda)A_{Si}(\lambda)\exp[-(1+i)a_Q(\omega)d_Q] + \eta_F(\lambda)A_F(\lambda)T_{Si}(\lambda)}{\eta_F(\lambda)A_F(\lambda)} \tag{6}$$

Under the realistic assumption [1] that $\eta_F(\lambda) \approx 1$ and, in view of the fact that $R_{Si}(\lambda)$ does not change by more than *ca.* 25% across the optical gap for a-$Si{:}H$ thin films [16,17], we set $A_{Si}(\lambda) = 1 - R_{Si}(\lambda) - T_{Si}(\lambda)$ $\approx 1 - T_{Si}(\lambda)$. This approximation, in practice, is not so bad as it may appear in the first place: neglecting $R_{Si}(\lambda)$ contributions for the sake of experimental PDS data interpretation has been previously successfully used [4] and has yielded optical absorption coefficient information within an error less than 20 %. Also, in view of the blackened PVDF detector surfaces, $A_F(\lambda) \approx 1$ to a very good approximation. Under these conditions, the low frequency P^2ES normalized signal becomes

$$S(\lambda,\omega) / S_R(\lambda,\omega) \approx \eta_{Si}(\lambda)[1 - T_{Si}(\lambda)] \exp[-(1+i)a_Q(\omega)d_Q] + T_{Si}(\lambda) \tag{7}$$

EXPERIMENTAL AND RESULTS

a-$Si{:}H$ thin films were prepared on quartz by plasma enhanced chemical vapor deposition (PECVD). The substate temperature was 225°C, total plasma power was 40 W, and the feeding gas was SiH_4 diluted to 10% in Helium. The gas flow rate was 200 sccm and the total gas pressure was 400 mTorr. The quartz substrates had been sputtered clean in Argon prior to deposition and were mounted at the anode of the PECVD system.

With regard to the P^2E spectrometer, excitation was provided by a 1000 W Xenon lamp coupled to a monochromator. An oscillating mirror was employed to alternately illuminate the reference and sample-holder cells. Both cells were fabricated using standard commercially available components as described elsewhere [18]. The surfaces of the 28 μm thick PVDF films were blackened so as to minimize the film reflectance $R_F(\lambda)$, which was shown to vary substantially for $Ni-Al$ electrodes [19] across the spectral range of interest (500-900 nm). The signal quality was improved substantially by using two Ithaco 1201 low-noise pre-amplifiers and appropriate frequency bandpass settings before channeling the photopyroelectric signals to lock-in amplifiers.

For purposes of comparison, a quartz cuvette containing an a-$Si{:}H$ sample was filled with water and substituted for the sample PVDF detector cell. A He-Ne laser probe beam was added and conventional normalized PD spectra were obtained using a standard position sensor (UDT Model 431 Position Monitor connected to a UDT SC125 light position detector) fitted with a narrowband optical filter at 632.8 nm. PDS signal normalization was performed through ratioing by the reference cell P^2E signal. The PDS signal quality was further enhanced using an Ithaco 1201 pre-amplifier stage in the same manner as with the P^2ES signal processing.

Figs. 1a and b show normalized P^2E spectra obtained at 20 and 0.9 Hz. The low energy end interference fringe patterns essentially coincide for both frequencies, in agreement with the highly transparent nature of the sample in that region where direct optical transmission is the cause of P^2E signal generation. At the high energy end of the spectrum, transmission-related signals are only of minor importance and contribute little in the thermally thin limit (0.9 Hz). The major contributor to the thermally thin signal is the transmission of the thermal wave generated within the *Si* film, which is acting as a heating strip on the surface of the much thicker quartz substrate. Also, Figs. 1a and b show the incoherent form of the data; in order to get the data into this form, suitable for analysis with Eq. (5), the following steps were utilized: a) The maximum transmittance was calculated theoretically, assuming $k(\lambda) = 0$, from

$$T_{max} = 4n_o n_Q/(n_o + n_Q)^2 = 0.96 \tag{8}$$

b) The lowest energy experimental interference fringe maximum was scaled to a value of 0.96, matching the theoretical T_{max}; c) The incoherent transmission was calculated from the envelope of extrema as the geometric average [20], $T_I = (T_{max}\, T_{min})^{1/2}$. d) Eq. (5) was used in the form

$$(T_I^{max})_{th} = 4n_o n_Q n/(n^2 + n_o n_Q)(n_o + n_Q) = (T_I^{max})_{exp} \tag{9}$$

for $k(\lambda) = \alpha(\lambda) = 0$, where $(T_I^{max})_{exp}$ is the value obtained from the flat portion of the P^2E transmission spectrum, or from the largest measured λ; e) Eq. (9) was finally solved for n:

$$n = 0.5(b + \sqrt{b^2 - 4c})\ ; \quad b \equiv \frac{4n_o n_Q}{(n_o + n_Q)T_I^{max}} \quad c \equiv n_o n_Q \tag{10}$$

Using $T_I^{max} = 0.596$ (obtained from Fig. 1b), Eq. (10) yields $n = 3.61$. This value for n is well within the band of accepted values for a-*Si*:*H* thin films [6,21]. It was assumed to be spectrally constant (also a standard thin-film PDS assumption [4]), and was subsequently used in all further calculations. Fig. 2 shows the optical absorption coefficient $\alpha(\lambda)$ spectrum obtained using the incoherent approximation of Fig. 1b as

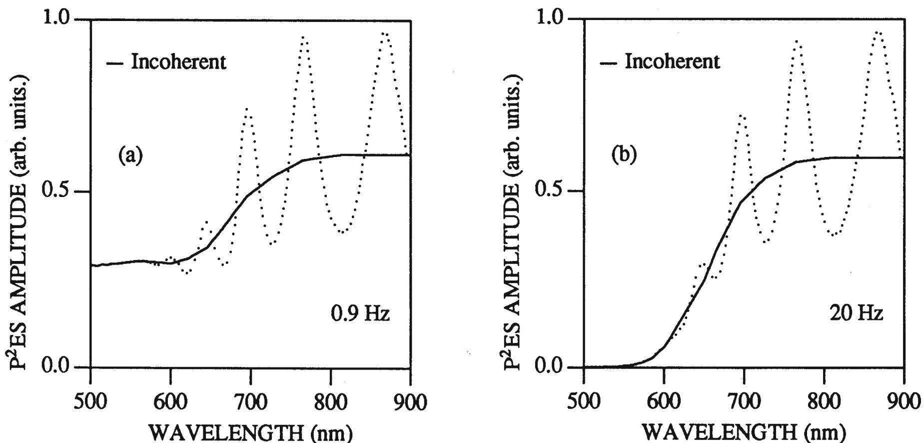

Fig. 1 P^2E spectra of a-*Si*:*H* thin film in the thermally thin (a) and thermally thick (b) case. The incoherent curve in (b) was used as $T_{Si}(\lambda)$ in Eq. (5). Slit-width resolution: 16 nm.

$T_{Si}(\lambda)$ in Eq. (5) (with $n = 3.61$). The values for $\alpha(\lambda)$ were obtained using the numerical method of halving the interval (or bisection method) [2]. For these calculations, the a-*Si:H* thin film thickness was estimated from the interference pattern of Fig. 1 using the approximate formula (n = constant) [23]

$$d_{Si} = \frac{1}{2n}\left[\frac{\lambda_{m+1}\lambda_m}{\lambda_{m+1}-\lambda_m}\right] \approx 0.9\mu m \tag{11}$$

where λ_{m+1}, λ_m correspond to adjacent interference maxima such that $\lambda_{m+1} > \lambda_m$.

Fig. 2 also shows the $\alpha(\lambda)$ spectrum obtained using conventional PDS. Assuming complete photothermal saturation at 500 nm, the normalized PDS signal may be divided by its saturation value yielding [24]

$$\frac{PDS(\lambda)}{PDS(\lambda_{saturation})} = \left[\frac{\eta_{Si}(\lambda)}{\eta_{Si}(\lambda_{saturation})}\right](1 - \exp[-\alpha(\lambda)d_{Si}]) \tag{12}$$

The PD $\alpha(\lambda)$ spectrum of Fig. 2 was obtained by smoothing the raw PDS signal output to eliminate the interference fringes, using a three-point averaging technique which was found very useful in previous work [25]. In addition, the simplifying assumption $\eta_{Si}(\lambda)/\eta_{Si}(\lambda_{saturation}) = 1$ was made, in line with conventional PDS spectroscopic calculations of thin films [4]. The similarity of the two entirely independently obtained $\alpha(\lambda)$ curves in Fig. 2 is remarkable and is a proof of the good spectroscopic capabilities of both techniques in measuring optical absorption. Fig. 2 shows that the assumption of saturation at $\lambda = 500$ nm is justified, in retrospect, as $1 - \exp[-\alpha(500\ nm)d_{Si}] \approx 1 - \exp(-7) \approx 1$. It ought to be noticed, however, that the PDS absorption curve falls consistently under the P^2ES curve throughout the measured spectral region. It will be seen below that the most likely source of this discrepancy is the non-constancy of $\eta_{Si}(\lambda)$.

The incoherent curve in Fig. 1a was then used for the self-consistent calculation of the nonradiative quantum efficiency $\eta_{Si}(\lambda)$. The thermally thin limit Eq. (7) indicates that, given experimental values for $T_{Si}(\lambda)$ (high-frequency P^2ES signal at incoherent approximation), and a good knowledge of d_Q and $a_Q(\omega)$, $\eta_{Si}(\lambda)$ may be calculated self-consistently for each wavelength using the amplitude of the low-frequency P^2ES signal. From a measurement of the frequency dependence of the P^2ES signal in the opaque region one can obtain a value for β_Q from the slope of the $Ln[S(\lambda,\omega) / S_R(\lambda,\omega)]$ vs. $\omega^{1/2}$ line (see Eq. (14)). Our measurement yielded the value $\beta_Q = 7.85 \times 10^{-3}$ cm^2/s for the quartz thermal diffusivity, in good agreement with published values [26]. Finally, Eq. (7) was solved for $\eta_{Si}(\lambda)$ in the form

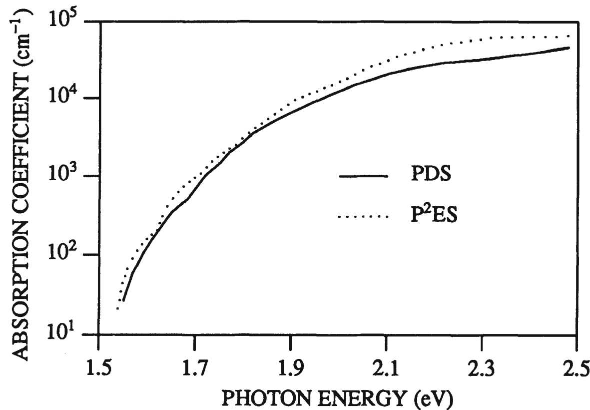

Fig. 2 Optical absorption coefficient calculation for a-*Si:H* thin film using P^{2}ES and PDS. For details see text.

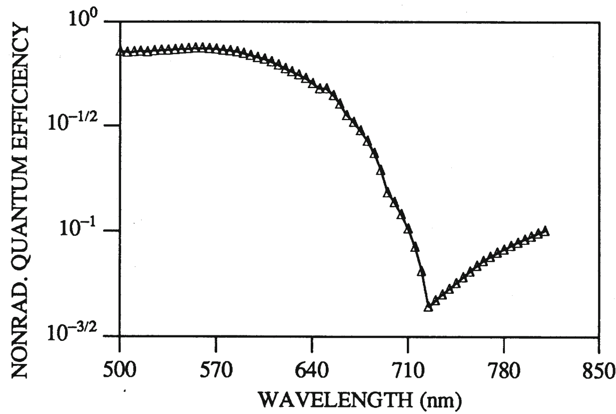

Fig. 3 Nonradiative quantum efficiency spectrum of a-*Si*:*H* thin film.

$$\eta_{Si}(\lambda) = \frac{\exp(a_Q d_Q)}{1 - T_{Si}(\lambda)}[\{[S(\lambda,\omega) / S_R(\lambda,\omega)]^2 - T_{Si}^2(\lambda)\sin^2(a_Q d_Q)\}^{1/2} - \cos(a_Q d_Q)] \tag{13}$$

The resulting $\eta_{Si}(\lambda)$ spectrum is shown in Fig. 3. The nonradiative quantum efficiency of the a-*Si*:*H* thin film sample is seen to vary by more than one order of magnitude across the material optical gap. It saturates at wavelengths above the gap, becoming independent of $h\nu$, as reported elsewhere [6], and decreases for below the gap excitation, in agreement with indirect (photoluminescence) measurements performed previously [27,28]. The increase in $\eta_{Si}(\lambda)$ for $\lambda \geq 720$ nm is not entirely understood at this time, however, it is associated with the discontinuity in the P^2E $\alpha(\lambda)$ curve at the same wavelength in Fig. 2. Fig. 3 indicates that the PDS assumption that $\eta_{Si}(\lambda) \approx \eta_{Si}(\lambda_{saturation})$ is not valid, and the fact that $\eta_{Si}(\lambda) < 1$ throughout the spectral range of interest is responsible for the lower effective absorption coefficient values calculated *via* PDS.

DISCUSSION

The P^2E optical absorption coefficient data of Fig. 2 may be understood largely in terms of amorphous *Si* thin film physics. Assuming a parabolic conduction band density of states approximation for non-direct optical transitions (i.e. a constant dipole interaction matrix element), the behavior of the optical absorption coefficient is given by [29]

$$\alpha(h\nu) = F(h\nu - E_G)^2 / n(h\nu)\, h\nu \tag{14}$$

where F is a constant, and E_G is the characteristic energy of the distribution of electronic states in bandlike regions (i.e. the optical gap). Fig. 4a shows the appropriately plotted data and an estimated $E_G = 1.7eV$ from the intercept of the (least-squares fitted) straight line to the data. This value of E_G is within the spread of previously reported values [16]: 1.6 - 1.7 eV. The low energy tail of the spectrum in Fig. 2 may also be explained in terms of an exponential valence-band density of states (Urbach tail) approximation [29]:

$$\alpha(h\nu) = G \exp(h\nu / E_o) \tag{15}$$

where G is a constant, and E_o is the characteristic energy of the distribution of electronic states in the tail-like region. Plotting the P^2ES data as shown in Fig. 4b and calculating the slope, one finds the value E_o

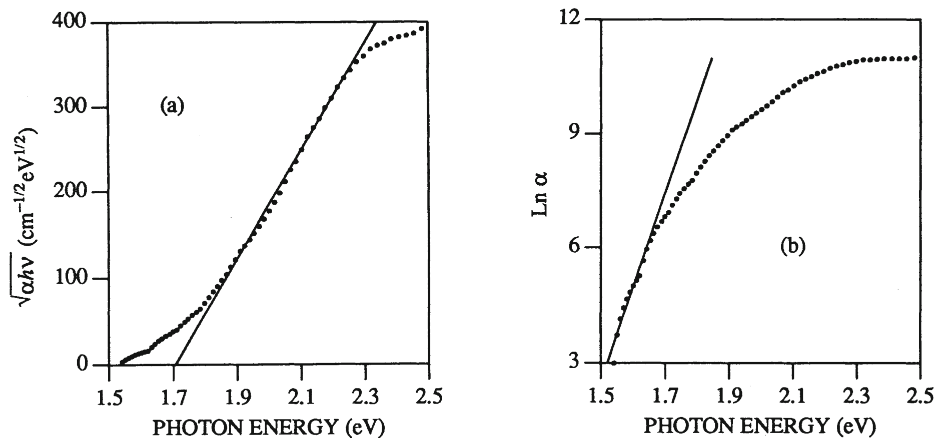

Fig. 4 Optical absorption coefficient P^2E spectrum plotted to illustrate: a) the $(\alpha h\nu)^{1/2}$ dependence on $h\nu$, and b) the $\ln\alpha$ dependence on $h\nu$.

≈ 41 *meV*. This value is well within the spread of previously reported values [16]: 25-80 meV. The good agreement of the absorption-tail P^2E signal-derived E_o value with an Urbach tail interpretation, i.e. a disorder-induced tailing off of defect states into the optical gap [30], is consistent with the increase in the nonradiative quantum efficiency in that region, Fig. 3: the disordered nature of the subgap defect states in the a-*Si:H* thin film sample is expected to show enhanced optical-to-thermal energy conversion activity. Such defects have previously been hypothesized to be the cause of luminescence quenching [31]. The direct $\eta_{Si}(\lambda)$ evidence provided in this work indicates, in agreement with this hypothesis, that the preferred subgap de-excitation channel is predominantly nonradiative, at the expense of other energy transfer processes. Clearly more work is needed to fully understand the implications of the subgap spectral dependence of $\eta_{Si}(\lambda)$ in Fig. 3. P^2ES appears to be a photothermal technique capable of producing *direct* $\eta(\lambda)$ spectra for the first time. This capability is expected to be an important vehicle to study in detail nonradiative de-excitation physics of amorphous semiconducting thin films.

CONCLUSIONS

In this work, P^2ES was shown to be capable of providing a-*Si:H* thin-film $\alpha(\lambda)$ and $\eta(\lambda)$ spectra directly and self-consistently from measurements at two modulation frequencies (thermally thick and thermally thin limits). Comparison of P^2ES $\alpha(\lambda)$ spectra with conventional PDS-obtained data showed that both techniques yield high quality results, however, PDS-extracted values tend to be underestimates due to non-unity values for $\eta(\lambda)$. Therefore, P^2ES appears to be very promising for amorphous thin film work. Its main advantages over conventional PDS are a) the absence of the solid-liquid interface, which is an undesirable feature for the characterization of optoelectronically active surfaces; and b) the direct spectroscopic measurement of the nonradiative quantum efficiency, an important quantity for the quality control and characterization of optoelectronic materials and devices.

ACKNOWLEDGMENTS

This work was supported by the Ontario Laser and Lightwave Research Center and the National Science and Engineering Research Council (NSERC) of Canada. The assistance of Linda Gowman and Gordon Verdin during the early stages of this work are gratefully acknowledged.

REFERENCES

1. H. Coufal, Appl. Phys. Lett. *45*, 516 (1984).
2. K. Tanaka, in *Photoacoustic and Thermal Wave Phenomena in Semiconductors*, edited by A. Mandelis (North-Holland, New York, 1987); Chap. 16; K. Tanaka, Y. Ichimura, and K. Sindoh, J. Appl. Phys. *63*, 1815 (1988).
3. A. Mandelis and M.M. Zver, J. Appl. Phys. *57*, 4421 (1985).
4. N.M. Amer and W.B. Jackson, in *Semiconductors and Semimetals, Vol. 21B*, edited by J.I. Pankove (Academic Press, New York, 1984); Chap. 3.
5. M. Kitamura, T. Ogawa, and T. Arai, J. Phys. Soc. Jpn *52*, 2561 (1983).
6. S. Yamasaki, Phil. Mag. B, *56*, 79 (1987).
7. A.F.S. Penna, J. Shah, A.E. DiGiovanni, A.Y. Cho, and A.C. Gossard, Appl. Phys. Lett. *47*, 591 (1985).
8. J.D. Winefordner and M. Rutledge, Appl. Spectrosc. *39*, 377 (1985).
9. W.B. Jackson, N.M. Amer, A.C. Boccara, and D. Fournier, Appl. Opt. *20*, 1333 (1981).
10. L.C. Aamodt and J.C. Murphy, J. Appl. Phys. *52*, 4903 (1981).
11. F. Abeles, in *Advanced Optical Techniques*, edited by A.C.S. van Heel (North-Holland, Amsterdam, 1967); Chap. 5.
12. R.E. Denton, R.D. Campbell, and S.G. Tomlin, J. Phys. D: Appl. Phys. *5*, 852 (1972).
13. J.C. Manifacier, J. Gasiot, and J.P. Fillard, J. Phys. E: Sci. Instrum. *9*, 1002 (1976).
14. T.C. Paulick, Appl. Opt. *25*, 562 (1986).
15. K.A. Epstein, D.K. Misemer, and G.D. Vernstrom, Appl. Opt. *26*, 294 (1987).
16. G.D. Cody, in *Semiconductors and Semimetals, Vol. 21B*, edited by J.I. Pankove (Academic Press, New York, 1984); Chap. 2.
17. D.T. Pierce and W.E. Spicer, Phys. Rev. B *5*, 3017 (1972).
18. H.J. Coufal, R.K. Grygier, D.E. Horne, and J.E. Fromm, J. Vac. Sci. Technol. A *5*, 2875 (1987).
19. PVDF Kynar[R] film with standard Ni-Al electrodes were purchased from Pennwalt Corp., Piezo Film Dept., 950 Forge Avenue, Valley Forge, PA. 19482.
20. K. Driss-Khodja, A. Gheorghiu, and M.-L. Theye, Opt. Commun. *55*, 169 (1985).
21. S.K. Bahl and S.M. Bhagat, J. Non-Cryst. Solids *17*, 409 (1975).
22. C.F. Gerald, *Applied Numerical Analysis, 2nd Ed.* (Addison-Wesley, Reading, 1980); p. 3.
23. A. Mandelis, E.K.M. Siu and S. Ho, Appl. Phys. A *33*, 153 (1984).
24. A. Mandelis, J. Appl. Phys. *54*, 3404 (1983).
25. T. Dioszeghy and A. Mandelis, J. Phys. Chem. Solids *47*, 1115 (1986); D.D. McCracken and W.S. Dorn, *Numerical Methods and FORTRAN Programming* (Wiley, New York, 1964).
26. A.C. Bento, H. Vargas, M.M.F. Aguiar and L.C.M. Miranda, Phys. Chem. Glasses *29*, 127 (1987).
27. R.A. Street, Phys. Rev. B. *21*, 5775 (1980).
28. M. Tajima, S. Yamasaki, H. Okushi, and K. Tanaka, Phys. Rev. B *33*, 8522 (1986).
29. M.H. Brodsky, R.S. Title, K. Weiser, and G.D. Pettit, Phys. Rev. B *1*, 2632 (1970).
30. N.F. Mott, Advan. Phys. *16*, 49 (1967).
31. W.B. Jackson and N.M. Amer, Phys. Rev. B *25*, 5559 (1982).